Chapter 4
NMR Explorations of Biomolecular Systems with Rapid Conformational Exchanges

Maho Yagi-Utsumi, Takumi Yamaguchi, Ryo Kitahara, and Koichi Kato

Abstract Biomolecules such as proteins and oligosaccharides undergo dynamic conformational exchanges, which are relevant to regulation of biologically functional processes as typified by molecular recognition. Nuclear magnetic resonance (NMR) spectroscopy provides useful approaches to characterize the conformational dynamics of biomolecules over a broad range of time scales. However, detailed characterizations of individual conformers are inherently challenging for those biomolecules that exhibit rapid conformational interconversions. Here we describe several NMR strategies to deal with dynamic conformational equilibria and ensembles using monomeric and dimeric ubiquitin (Ub) and the oligosaccharide moieties of gangliosides as model molecules. A specific Ub conformer could be enriched using high pressure combined with a single amino acid substitution. Introducing a covalent linkage constrained the conformational states of a Ub dimer. NMR spectroscopy was also useful for validating molecular dynamics simulations of highly flexible oligosaccharides. These methods provided for detailed determinations of dynamic conformational exchanges that involve minor conformational species.

M. Yagi-Utsumi
Okazaki Institute for Integrative Bioscience and Institute for Molecular Science, National Institutes of Natural Sciences, 5-1 Higashiyama, Myodaiji, Okazaki 444-8787, Japan

Graduate School of Pharmaceutical Sciences, Nagoya City University, 3-1 Tanabe-dori, Mizuho-ku, Nagoya 467-8603, Japan

Department of Chemistry, University of Cambridge, Lensfield Road, Cambridge CB2 1EW, UK

T. Yamaguchi • K. Kato (✉)
Okazaki Institute for Integrative Bioscience and Institute for Molecular Science, National Institutes of Natural Sciences, 5-1 Higashiyama, Myodaiji, Okazaki 444-8787, Japan

Graduate School of Pharmaceutical Sciences, Nagoya City University, 3-1 Tanabe-dori, Mizuho-ku, Nagoya 467-8603, Japan
e-mail: kkatonmr@ims.ac.jp

R. Kitahara
College of Pharmaceutical Sciences, Ritsumeikan University, 1-1-1 Noji-higashi, Kusatsu 525-8577, Japan

M. Terazima et al. (eds.), *Molecular Science of Fluctuations Toward Biological Functions*, DOI 10.1007/978-4-431-55840-8_4

Keywords Nuclear magnetic resonance spectroscopy • Conformational exchange • Ubiquitin • Oligosaccharides • Molecular dynamics simulation

4.1 Introduction

As a part of living systems, biomacromolecules are characterized by their various degrees of freedom with regard to internal motions, which provide them with conformational plasticity that is required during binding and reaction processes and also for conformational adaptability to their binding partners. For example, many proteins exhibit multiple conformations in the absence of their cognate ligands, which select and stabilize specific conformers of the target proteins [1, 2]. Conformational dynamics during molecular recognition processes are exemplified by intrinsically disordered proteins that are devoid of stable secondary or tertiary structures and are often folded into specific secondary structures upon interacting with their binding partners [3, 4].

Nuclear magnetic resonance (NMR) spectroscopy provides potentially useful tools for characterizing the conformational dynamics of biomolecules over a wide range of time scales (Fig. 4.1) [5, 6]. If the conformational interconversion is sufficiently slow on the NMR time scale, then NMR signals originating from individual conformers are observable and provide detailed information for each conformational state. However, under circumstances when conformational transitions occur faster, the NMR peaks converge at a position that corresponds to a population-weighted average of chemical shifts. Even under these conditions, NMR relaxation dispersion experiments can provide information on a chemical shift and a population of conformers as well as the exchange rate if the interconversion occurs on the micro-to-millisecond time scale [7–9].

Conformational fluctuations on the subnanosecond time scale are characterized based on measurements of longitudinal and transverse relaxation rates (R_1 and R_2, respectively) and the heteronuclear Overhauser effect (NOE). For example, a model-free formalism is widely used to describe protein backbone dynamics with order parameters and correlation times of individual amino acid residues on the basis of observations of ^{15}N R_1, R_2, and $\{^1\text{H}\}$-^{15}N NOE [10, 11]. However, it is challenging to characterize individual conformers that form such a dynamic ensemble of biomolecules.

In this chapter, we present several examples of strategies for obtaining detailed information on specific conformers under dynamic equilibrium, particularly minor conformational species under physiological conditions.

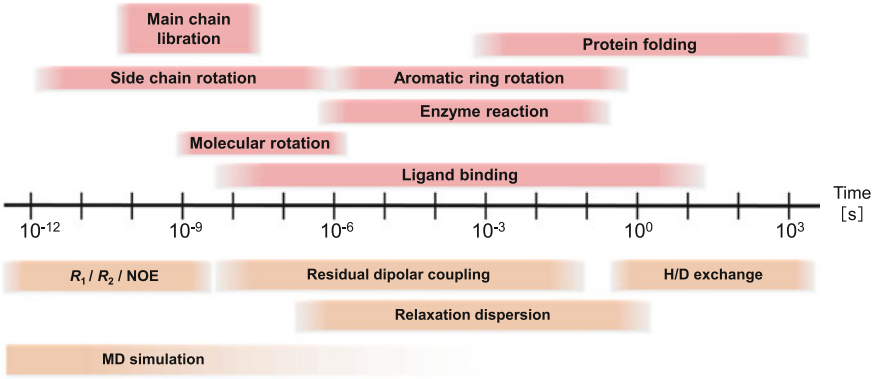

Fig. 4.1 Biomolecular NMR experiments to characterize protein dynamics on different time scales

4.2 Trapping Conformational States

4.2.1 High-Pressure NMR Combined with a Mutational Approach

In many biomolecular NMR studies, spectral measurements are made under equilibrium solution conditions in which the molecules undergo dynamic conformational interconversions. Among pre-existing conformers, major conformers are not always biologically active. For detailed structural analyses of their minor conformational states, the equilibria are perturbed by changing solution conditions, such as the pH, salt concentration, and temperature, so as to make the originally minor species more populated.

High-pressure NMR spectroscopy is one of the most powerful methods for capturing low-population conformational species of proteins, which have higher Gibbs free energies than their basic folded state (native state). Because the conformational fluctuations of a protein in solution are closely related to the fluctuations of its partial molar volume [12, 13], applying high pressure causes a population shift of conformers within the ensemble, which results in NMR spectral changes [14]. Here we illustrate the utility of the high-pressure NMR approach using ubiquitin (Ub) as a model.

Ub is a small protein that consists of 76 amino acid residues and is a posttranslational protein modifier, which plays crucial regulatory roles in diverse cellular events [15]. A Ub modification can be made through the formation of isopeptide linkages at its C-terminus. Although Ub can be covalently attached to target proteins in a monomeric form, it can also be linked to another Ub to generate various types of polyUb chains. PolyUb chains that are mediated through a Lys48 isopeptide linkage provide a signal that is recognized by the 26S proteasome for selective protein degradation in cells. The formation of Ub isopeptide linkages is

catalyzed by three enzymes, Ub-activating enzyme E1, Ub-conjugating enzyme E2, and Ub-protein ligase E3, in sequential order.

Previously reported high-pressure NMR investigations demonstrated that Ub existed in equilibrium among its natively folded state N_1, a totally unfolded state U, and at least two high-energy states, an alternatively folded state N_2 and a locally disordered state I [16–18]. Based on spectral data acquired at low (30 bar) and high (3 kbar) pressures, it was concluded that the N_2 state accounted for 77 % of the population at high pressure, which involved reorientation of its C-terminal β_5-strand and α_1-helix and provided an open conformation in the proximity of its C-terminus [18]. The structural changes of pressure-stabilized N_2 were supported by residual dipolar coupling (RDC) experiments [19] and 1 μs molecular dynamics (MD) simulations [20] of the protein under high pressure.

We demonstrated that the high-pressure NMR approach provided a new strategy for amplifying particular fluctuations in proteins by rational mutation designed based on the conformational states observed under different pressure conditions [21]. With this strategy, the N_1 (30 bar) and N_2 (3 kbar) structures of wild-type (WT) Ub were first compared to identify the key intramolecular interactions. Subsequently, the hydrogen bond or salt bridge thus identified was systematically broken by single amino acid replacements to control conformational fluctuations. A series of Ub mutants (K11A, E34A, Q41A, and Q41N) were subjected to heteronuclear single-quantum coherence (HSQC) experiment-based chemical shift comparisons (Fig. 4.2), which indicated that the Q41N mutant preferentially (70 %) adopted the N_2 conformation at atmospheric pressure. The NMR structure of the N_2 conformer of Q41N-mutated Ub determined at atmospheric pressure confirmed that the hydrogen bond between the Ile36 backbone carbonyl group and the Gln41 side chain amide group was critical for controlling the N_1-N_2 conformational interconversion in WT Ub.

In the Q41N mutant, the N_2 state accounted for 97 % of the population at high pressure (2.5 kbar), which enabled detailed conformational characterizations of the "pure" N_2 state of Ub [22]. The N_2 state exhibited an altered orientation of β_5-strand as compared with that of the natively folded N_1 state (Fig. 4.3). Interestingly, the conformation of N_2 was quite similar to the crystal structure of Ub in complex with the Ub-activating enzyme E1 (Fig. 4.4), which indicated that Ub recognition by E1 was best explained by conformational selection rather than induced-fit motion. Similar high-energy, biologically active states are shared by NEDD8, a Ub-like posttranslational modifier that has its own E1−E2−E3 reaction cascade [23]. These findings suggest that both the major ground state and the minor active conformational state are conserved among the Ub-like modifiers.

Thus, high-pressure NMR measurements combined with suitably chosen point mutations could be a useful strategy for conformational trapping of natively low-populated but functionally relevant protein states.

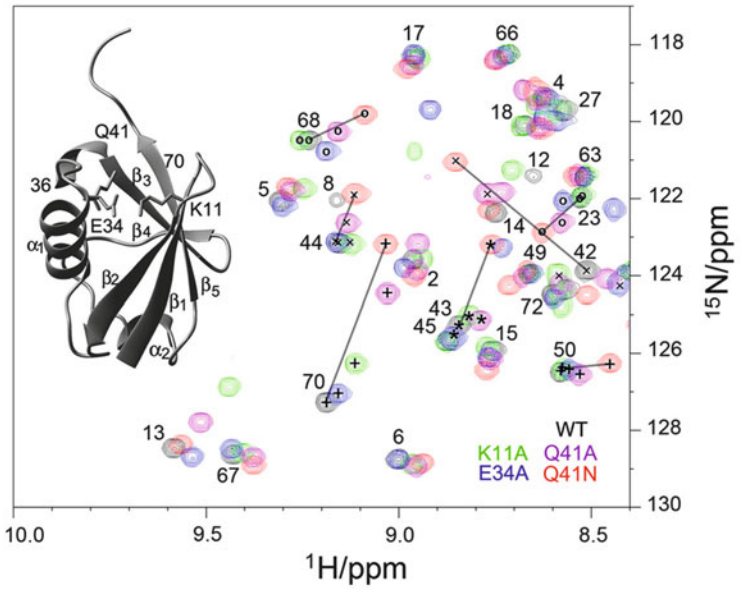

Fig. 4.2 Overlay of the HSQC spectra of WT (*black*) and mutated Ubs (K11A, *green*; E34A, *blue*; Q41A, *purple*; Q41N, *red*). The substituted side chains are shown in the inset Ub structure. All mutant peaks lie approximately in a straight line that connects the WT and Q41N peaks (Adapted with permission from Ref. [21])

4.2.2 Covalent Constraints of Biomolecular Conformations

Protein functions are derived primarily through the cooperative interplay between two or more domains. The plasticity in spatial arrangements of these domains is a key feature of multidomain proteins endowed with sophisticated molecular mechanisms typified by allosteric regulation. Interconversion of domain arrangements takes place over a wide range of temporal and spatial time scales. When domain rearrangements are rapid, it is again not possible to describe individual conformational states based on NMR data obtained as population-weighted averages unless specific conformers can be *frozen*. Here we present our results for characterizing the conformational dynamics of a Lys48-linked Ub dimer (diUb) by NMR spectroscopy in conjunction with X-ray crystallography [24].

The previously reported crystal structure of Lys48-linked diUb exhibited a compact closed conformation in which the hydrophobic surfaces in both Ub units were packed against each other and shielded from the solvent [25]. The Ub hydrophobic surface is involved in interactions with the Ub-binding proteins that function in the Ub-/proteasome-mediated protein degradation pathway, including the proteasome subunits Rpn10 and Rpn13 [26, 27]. Therefore, one may wonder how Ub-binding proteins can efficiently access the functionally important but sequestered hydrophobic surface of the Lys48-linked polyUb chains. We addressed

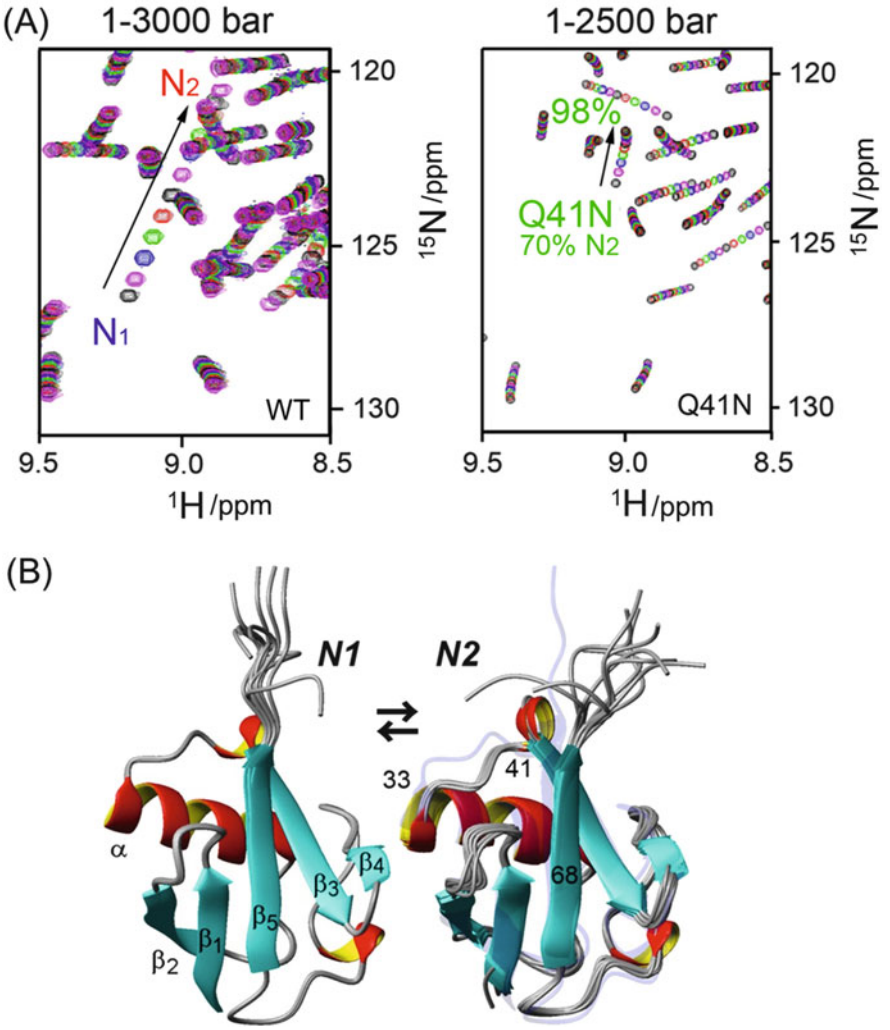

Fig. 4.3 (**a**) Superposition of HSQC spectra of WT (*left*) and Q41N (*right*) Ub at different pressures. The Q41N mutant preferentially (70 %) adopts the N_2 conformation at atmospheric pressure. (**b**) Solution structure of WT ubiquitin at 1 bar, a model for the basic folded conformation N_1 [Protein Data Bank (PDB) entry 1D3Z] (*left*), and the Q41N variant at 2500 bar, model for the alternatively folded conformation N_2 (PDB entry 2RU6) (*right*) (Adapted with permissions from Refs. [21] and [22])

this using Lys48-linked diUb prepared by in vitro E1–E2 (E2-25 K) enzymatic reactions [28], which generated WT Lys48-linked polyUb chains as well as their cyclic forms, in which each Ub unit was linked *via* two isopeptide linkages (Fig. 4.5). Chromatographically isolated WT and cyclic Lys48-linked diUb were then subjected to structural analyses.

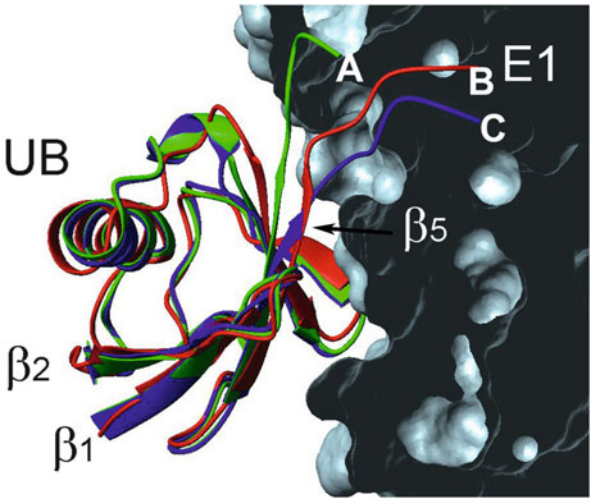

Fig. 4.4 Superposition of NMR-derived structures of WT Ub at 1 bar (*green*, PDB entry 1D3Z) and Q41N at 2500 bar (*red*, PDB entry 2RU6) on the crystal structure of the Ub−E1 complex (*blue*, PDB entry 3CMM). E1 is shown as a molecular surface (*gray*) (Adapted with permission from Ref. [22])

Intriguingly, our resolved crystal structure of WT Lys48-linked diUb exhibited an open conformation in contrast to the previously reported crystal structures and suggested that the crystallographic data provided snapshots of the diUb molecule under dynamic equilibrium in solution (Fig. 4.6a). Furthermore, our NMR-derived 3D structure of the cyclic diUb form closely resembled the closed conformation observed in the crystals (Fig. 4.6b). Thus, the closed conformer could be successfully *isolated* by introducing additional isopeptide linkages. Interestingly, endogenous cyclic Lys48-linked diUb was detected in skeletal muscle and cultured mammalian cells [29], although its physiological role remains unknown.

HSQC spectral data of WT Lys48-linked diUb were compared with those of the cyclic form and monomeric Ub, which mimics an open form of diUb in terms of its hydrophobic surface exposure (Fig. 4.7). In WT diUb, each amino acid residue located on the hydrophobic surface provided a single HSQC peak between the peaks that originated from the corresponding sites in monomeric Ub and cyclic diUb in the same straight line with an identical dividing ratio. These data demonstrated that Lys48-linked diUb interconverted between open and closed conformations, which were mimicked by monomeric Ub and cyclic diUb, respectively, in the fast-exchange regime. In this system, the populations of open and closed conformers were determined to be 75 % and 25 %, respectively, based simply on the division ratio of the chemical shift difference. The open conformation accounted for a greater population under lower pH conditions and almost completely predominated at pH 4.5 (Fig. 4.8). These data suggested that the intrinsic properties of Lys48-linked Ub chains to adopt the open conformation may be advantageous for their interactions with Ub-binding proteins.

This study demonstrates the utility of conformational trapping of multidomain proteins by introducing covalent linkage constraints.

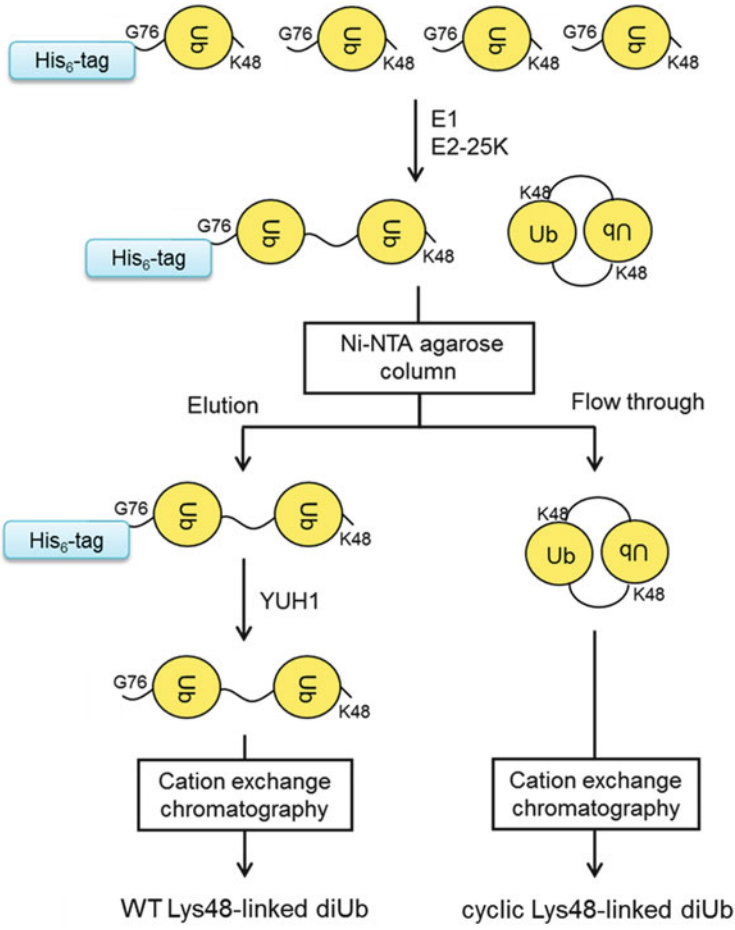

Fig. 4.5 Schematic diagram for preparing WT and cyclic Lys48-linked Ub chains (Adapted with permission from Ref. [24])

4.3 Exploration of Conformational Spaces of Flexible Biomolecules

In the previous sections, we described protein conformational dynamics as interchanges among a few conformers. However, in general, biomolecular dynamics involve not only conformational transitions from a low-energy minimum to another in the energy landscape but also harmonic motions in each energy minimum. This is particularly true for highly flexible biomolecules best represented by oligosaccharides and intrinsically disordered proteins. Oligosaccharides have branched structures and have numerous degrees of freedom of motion, which provide conformational spaces with a number of shallow and broad energy minima

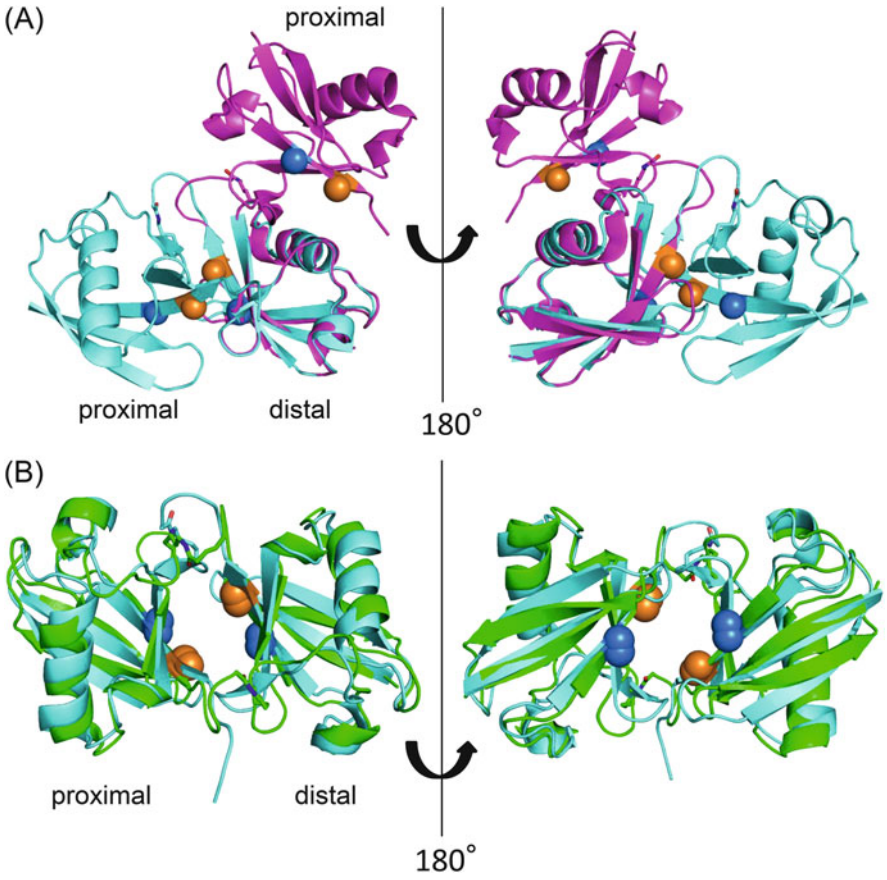

Fig. 4.6 (**a**) Superposition of the crystal structures of WT Lys48-linked diUb in the open (present structure; PDB code, 3AUL) (*magenta*) and closed forms (PDB code, 1AAR) (*cyan*). (**b**) Superposition of the NMR-derived model of cyclic Lys48-linked diUb (*green*) and the crystal structure of WT Lys48-linked diUb showing the closed conformation (PDB code, 1AAR) (*cyan*). The C-terminal group of Ub is linked to another Ub (designated the distal and proximal moieties, respectively) through its Lys48 side chain (Adapted with permission from Ref. [24])

[30]. Thus, the three-dimensional (3D) structure of such a flexible oligosaccharide should be interpreted as a vast ensemble of dynamic conformations, rather than only a limited number of conformational states.

The biological functions of oligosaccharides are exerted primarily through molecular recognition processes that are mediated by carbohydrate-binding proteins collectively designated lectins [31, 32]. For example, various high-mannose-type oligosaccharides attached to proteins serve as quality indicators in the early secretory pathway, which are recognized by a series of intracellular lectins that function during protein folding, transport, and degradation processes [33–35]. On cell surfaces, various glycoconjugates mediate a number of physiological and

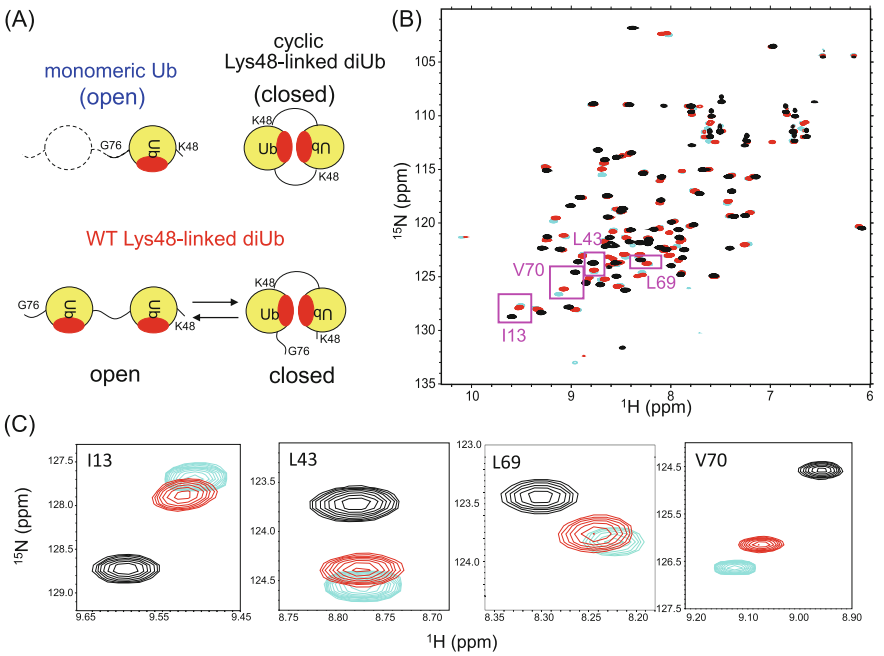

Fig. 4.7 (**a**) Cartoon model of the conformational equilibrium of WT Lys48-linked diUb. Cyclic Lys48-linked diUb was used as a mimic of the closed state, and monomeric Ub was used as a mimic of the open state. The hydrophobic surface is colored red. (**b**) ^{1}H–^{15}N HSQC spectra of monomeric Ub (*cyan*), WT Lys48-linked diUb (*red*), and cyclic Lys48-linked diUb (*black*) at pH 7.0. (**c**) Close-up views of the spectral regions (*boxed*), including the peaks for Ile13, Leu43, Leu69, and Val70, are displayed at the bottom (Adapted with permission from Ref. [24])

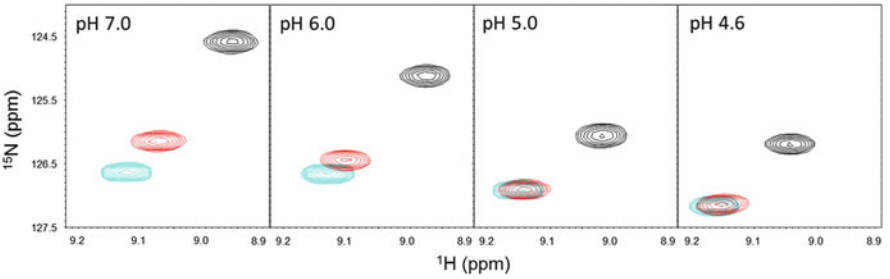

Fig. 4.8 pH-dependent chemical shift changes of the HSQC peaks for monomeric Ub (*cyan*), WT Lys48-linked diUb (*red*), and cyclic Lys48-linked diUb (*black*), which shows that the open conformation of WT Lys48-linked diUb becomes populated upon lowering the pH (Adapted with permission from Ref. [24])

pathological processes, as exemplified by gangliosides, glycosphingolipids containing sialyl residue(s), which are involved in cellular communications and development, cancer metastasis, viral infections, and the onset and progression of neurodegenerative disorders [36–39].

To better understand the mechanisms underlying oligosaccharide functions, their 3D structural information should be acquired with quantitative descriptions of their dynamic, rapid conformational fluctuations. NMR methods combined with computational simulation techniques provide useful tools to explore the conformational spaces of flexible biomolecules. For example, MD simulations can be used to predict the dynamic conformational motions of highly flexible oligosaccharides in solution [40, 41]. However, a frequent problem with this approach is its dependence on simulation protocols, including initial structures, computational times, and the choice of force fields. Therefore, it is critically important to validate the simulation results by comparisons with experimental data for biomolecular fluctuations on time scales ranging from subnanoseconds to microseconds. We developed a methodology to evaluate MD simulation results using paramagnetism-assisted NMR techniques to explore the conformational spaces occupied by flexible oligosaccharides in solution [42].

Introducing a paramagnetic center, such as lanthanide ions, into a target biomolecule results in significant modifications of its NMR spectra due to the generated magnetic dipole–dipole interactions between nuclei and an unpaired electron [43, 44]. For example, pseudocontact shift (PCS), a well-known paramagnetic effect observed in the presence of lanthanide ions with anisotropic magnetic susceptibility, can modulate the chemical shift of each NMR signal according to the spatial arrangements of individual nuclei with respect to the paramagnetic center [45]. Because of the large magnetic moment of unpaired electrons, through-space dipole interactions perturb not only the signals from the nuclei in proximity to the paramagnetic center but also those that are distal from it. Thus, PCS measurements have the potential to provide valuable atomic long-distance information for characterizing biomolecular conformations.

We applied this method to evaluate the conformational dynamics of a GM3 trisaccharide (NeuAcα2-3Galβ1-4Glc), the common core oligosaccharide structure shared among gangliosides [46]. Attaching a paramagnetic lanthanide tag to this trisaccharide allowed us to measure PCS effects (Fig. 4.9a). Using two-dimensional ^{1}H–^{13}C HSQC spectra, the PCS values of each ^{1}H and ^{13}C nucleus were acquired as the differences in chemical shifts between the oligosaccharide tagged with a paramagnetic ion, such as Tm^{3+}, and that modified with a diamagnetic reference La^{3+} ion (Fig. 4.9b). Because the 3D structure of the oligosaccharide rapidly fluctuates in solution, the observed PCS data should be interpreted as averages over the dynamic conformational ensemble. Thus, we performed MD simulations in explicit water to create a vast conformational ensemble of this oligosaccharide. The simulation results showed wide distributions of torsion angles in this trisaccharide, particularly around a glycosidic linkage between the NeuAc and Gal residues (Fig. 4.10). From the computed trajectory of the trisaccharide over a total of 120 ns, 2000 conformers were sampled, which involved harmonic motions

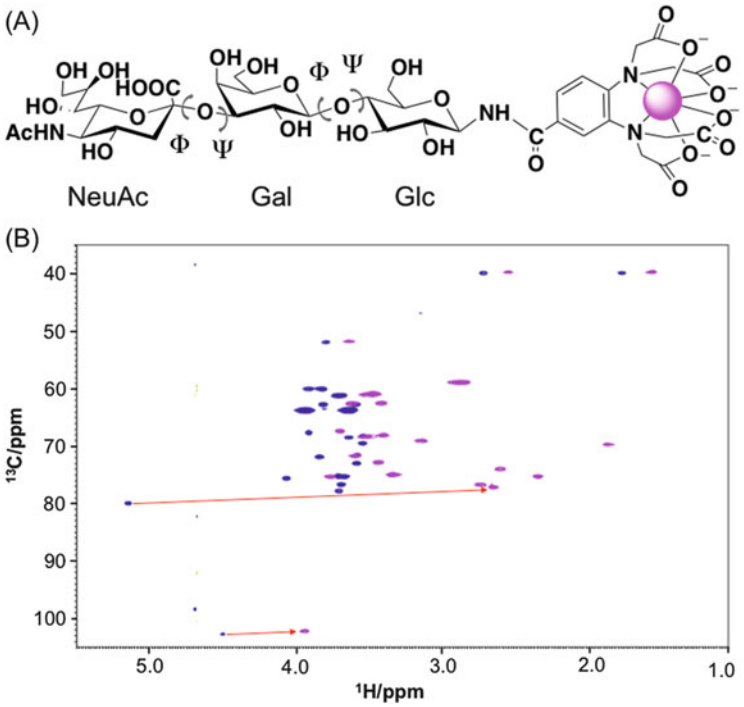

Fig. 4.9 PCS measurements for the GM3 trisaccharide. (**a**) Introducing a paramagnetic lanthanide tag. (**b**) ^{1}H–^{13}C HSQC spectra of the tagged oligosaccharide in complex with Tm^{3+} (*magenta*) and La^{3+} (*blue*). *Arrows* indicate chemical shift differences for the anomeric CH groups of Gal and Glc residues (Adapted with permission from Ref. [46])

in a local minimum as well as transitions from one low-energy region to another in the energy landscape.

Using the atomic coordinates generated from this dynamic ensemble model, the conformational space of the GM3 trisaccharide derived from the MD simulations was quantitatively validated. With this approach, the experimentally obtained PCS values were compared with those that were back calculated from the ensemble model. The results for the back-calculated PCS values were in excellent agreement with the experimental data with a small Q value (used as criteria for agreement between experimental and calculated values), which indicated successful exploration of the conformational spaces of this oligosaccharide (Fig. 4.11). Using most single conformers or using a combination of selected low-energy conformers gave compromised Q values. Furthermore, such a low Q value was not estimated from a conformational ensemble of this trisaccharide without considering its low-populated (around 2 %) conformational cluster (Figs. 4.10 and 4.11). These results underscore the existence of the minor conformers in solution and their significant contributions to the observed NMR data.

A unique structural feature of oligosaccharides is their branching with multiple modes of linkage, which provide diverse 3D structures. To examine the impact of

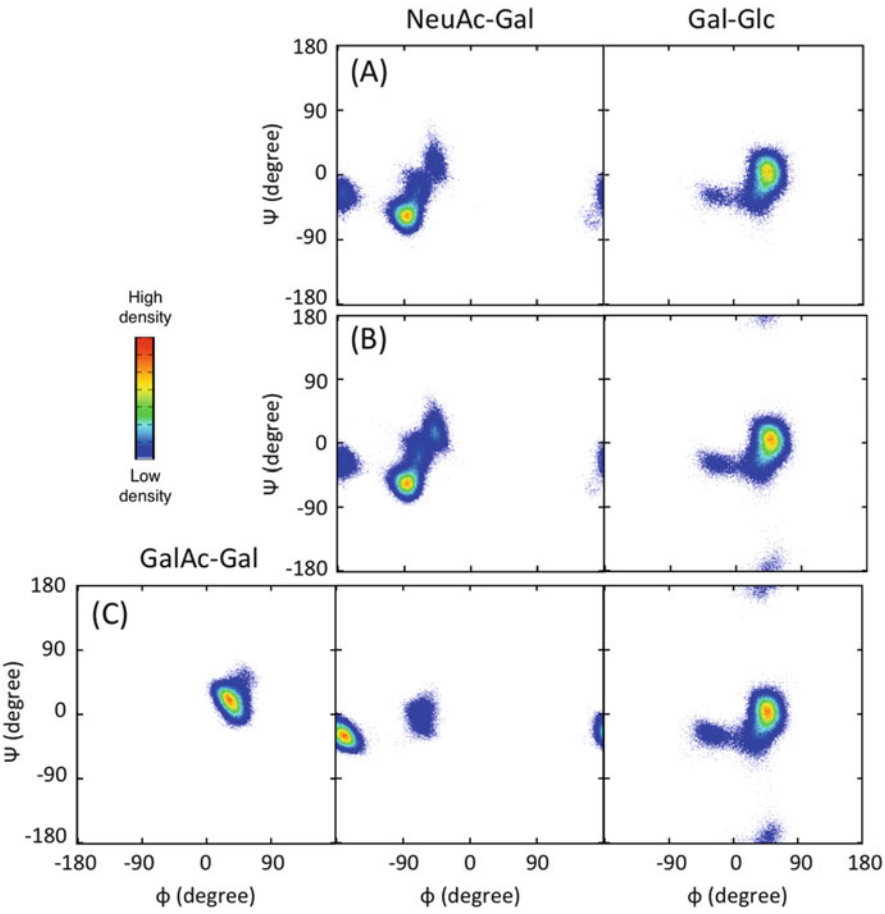

Fig. 4.10 Torsion angle density maps of the MD trajectory for the GM3 trisaccharide with a total simulation time of (**a**) 60 ns and (**b**) 120 ns and (**c**) the GM2 tetrasaccharide with a total simulation time of 120 ns (Adapted with permissions from Refs. [46] and [47])

these branches on the conformations and dynamics of oligosaccharides, paramagnetism-assisted NMR analyses in conjunction with MD simulations were also used to conformationally characterize a branched oligosaccharide, GM2 tetrasaccharide (GalNAcβ1-4[NeuAcα2-3]Galβ1-4Glc), which has an additional GalNAc branch as compared with the GM3 trisaccharide [47].

The PCS-validated conformational spaces of the GM2 and GM3 oligosaccharides showed similarities in their Gal–Glc glycosidic linkage conformations. In contrast, significant differences were observed between the GM2 and GM3 oligosaccharides in terms of the conformational spaces around the NeuAc–Gal glycosidic linkages (Fig. 4.10c). A corresponding cluster of this linkage to the most populated conformations in the GM3 trisaccharide was missing in the

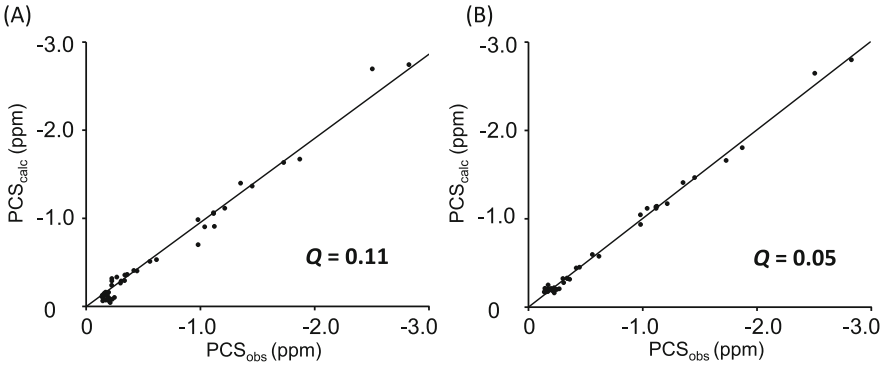

Fig. 4.11 Correlations between experimentally observed PCS values with Tm^{3+} and computationally calculated PCS data for the GM3 trisaccharide. The PCS values were back calculated from ensemble models derived from (**a**) the trajectory with a total simulation time of 60 ns and (**b**) those with a simulation time of 120 ns (Adapted with permission from Ref. [46])

conformational space of the GM2 tetrasaccharide. This suggests that in the biantennary GM2 tetrasaccharide, the additional GalNAc residue controls the conformational fluctuation of another branch. The corresponding NeuAc–Gal glycosidic linkage has conformational freedom in the linear GM3 oligosaccharide.

4.4 Concluding Remarks

In this chapter, we outlined two contrasting types of NMR approaches for characterizing individual conformers of biomolecules that rapidly interchange with one another. In one approach, a specific conformer is enriched or even isolated for detailed NMR analyses. Our NMR studies of mono- and diUb illustrated this conformational trapping by applying high pressure, point mutations, pH optimization, and covalent constraints. Crystallographic snapshots can also be used to interpret NMR data for a dynamic conformational ensemble. In another more systematic approach, the dynamic behaviors of biomolecules in solution can be directly observed by NMR-validated MD simulations. This method can be applied to describe dynamic pictures of flexible biomolecules, including intrinsically disordered proteins. Thus, sophisticated NMR spectroscopic techniques combined with X-ray crystallography and MD simulations provide versatile tools for characterizing the conformational dynamics of biomolecules and exploring their conformational spaces.

In living systems, these flexible biomolecules are self-organized into highly ordered supramolecular structures and, more importantly, are autonomously disassembled to create higher functions. For these systems, NMR spectroscopy provides valuable microscopic information on the local conformational dynamics of biomolecules during the processes involved in biomolecular organization, which

can be complemented by macroscopic information on the overall structures of these supramolecular complexes provided by solution scattering, electron microscopy, and other biophysical methods. In this context, NMR has important roles for exploring the dynamic ordering of biomolecular systems for the generation of integrated functions.

Acknowledgments This work was partly supported by the JSPS/MEXT Grants in Aid for Scientific Research on Innovation Areas (23107729, 20107004, and 25102008), Young Scientists (B) (25840025 and 24750170), and Challenging Exploratory Research (26560451) and by the Okazaki ORION project. M. Y. U. is a recipient of the Naito Foundation Grant for Studying Overseas.

References

1. Boehr DD, Nussinov R, Wright PE (2009) The role of dynamic conformational ensembles in biomolecular recognition. Nat Chem Biol 5:789–796
2. Lange OF, Lakomek NA, Fares C, Schroder GF, Walter KF, Becker S et al (2008) Recognition dynamics up to microseconds revealed from an RDC-derived ubiquitin ensemble in solution. Science 320:1471–1475
3. Mittag T, Kay LE, Forman-Kay JD (2010) Protein dynamics and conformational disorder in molecular recognition. J Mol Recognit 23:105–116
4. Uversky VN, Dunker AK (2010) Understanding protein non-folding. Biochim Biophys Acta 1804:1231–1264
5. Kleckner IR, Foster MP (2011) An introduction to NMR-based approaches for measuring protein dynamics. Biochim Biophys Acta 1814:942–968
6. Mittermaier AK, Kay LE (2009) Observing biological dynamics at atomic resolution using NMR. Trends Biochem Sci 34:601–611
7. Hansen DF, Vallurupalli P, Kay LE (2008) An improved ^{15}N relaxation dispersion experiment for the measurement of millisecond time-scale dynamics in proteins. J Phys Chem B 112:5898–5904
8. Loria JP, Rance M, Palmer AG (1999) A relaxation-compensated Carr−Purcell−Meiboom−Gill sequence for characterizing chemical exchange by NMR spectroscopy. J Am Chem Soc 121:2331–2332
9. Sugase K, Dyson HJ, Wright PE (2007) Mechanism of coupled folding and binding of an intrinsically disordered protein. Nature 447:1021–1025
10. Lipari G, Szabo A (1982) Model-free approach to the interpretation of nuclear magnetic resonance relaxation in macromolecules. 1. Theory and range of validity. J Am Chem Soc 104:4546–4559
11. Lipari G, Szabo A (1982) Model-free approach to the interpretation of nuclear magnetic resonance relaxation in macromolecules. 2. Analysis of experimental results. J Am Chem Soc 104:4559–4570
12. Gekko K, Hasegawa Y (1986) Compressibility-structure relationship of globular proteins. Biochemistry 25:6563–6571
13. Chalikian TV, Breslauer KJ (1998) Thermodynamic analysis of biomolecules: a volumetric approach. Curr Opin Struct Biol 8:657–664
14. Akasaka K (2003) Highly fluctuating protein structures revealed by variable-pressure nuclear magnetic resonance. Biochemistry 42:10875–10885
15. Hershko A, Ciechanover A (1998) The ubiquitin system. Annu Rev Biochem 67:425–479

16. Kitahara R, Yamada H, Akasaka K (2001) Two folded conformers of ubiquitin revealed by high-pressure NMR. Biochemistry 40:13556–13563
17. Kitahara R, Akasaka K (2003) Close identity of a pressure-stabilized intermediate with a kinetic intermediate in protein folding. Proc Natl Acad Sci U S A 100:3167–3172
18. Kitahara R, Yokoyama S, Akasaka K (2005) NMR snapshots of a fluctuating protein structure: ubiquitin at 30 bar-3 kbar. J Mol Biol 347:277–285
19. Fu Y, Wand AJ (2013) Partial alignment and measurement of residual dipolar couplings of proteins under high hydrostatic pressure. J Biomol NMR 56:353–357
20. Imai T, Sugita Y (2010) Dynamic correlation between pressure-induced protein structural transition and water penetration. J Phys Chem B 114:2281–2286
21. Kitazawa S, Kameda T, Yagi-Utsumi M, Sugase K, Baxter NJ, Kato K et al (2013) Solution structure of the Q41N variant of ubiquitin as a model for the alternatively folded N2 state of ubiquitin. Biochemistry 52:1874–1885
22. Kitazawa S, Kameda T, Kumo A, Yagi-Utsumi M, Baxter NJ, Kato K et al (2014) Close identity between alternatively folded state N2 of ubiquitin and the conformation of the protein bound to the ubiquitin-activating enzyme. Biochemistry 53:447–449
23. Kitahara R, Yamaguchi Y, Sakata E, Kasuya T, Tanaka K, Kato K et al (2006) Evolutionally conserved intermediates between ubiquitin and NEDD8. J Mol Biol 363:395–404
24. Hirano T, Serve O, Yagi-Utsumi M, Takemoto E, Hiromoto T, Satoh T et al (2011) Conformational dynamics of wild-type Lys-48-linked diubiquitin in solution. J Biol Chem 286:37496–37502
25. Cook WJ, Jeffrey LC, Carson M, Chen Z, Pickart CM (1992) Structure of a diubiquitin conjugate and a model for interaction with ubiquitin conjugating enzyme (E2). J Biol Chem 267:16467–16471
26. Varadan R, Assfalg M, Raasi S, Pickart C, Fushman D (2005) Structural determinants for selective recognition of a Lys48-linked polyubiquitin chain by a UBA domain. Mol Cell 18:687–698
27. Zhang N, Wang Q, Ehlinger A, Randles L, Lary JW, Kang Y et al (2009) Structure of the s5a: k48-linked diubiquitin complex and its interactions with rpn13. Mol Cell 35:280–290
28. Yao T, Cohen RE (2000) Cyclization of polyubiquitin by the E2-25K ubiquitin conjugating enzyme. J Biol Chem 275:36862–36868
29. Sokratous K, Strachan J, Roach LV, Layfield R, Oldham NJ (2012) Cyclisation of Lys48-linked diubiquitin in vitro and in vivo. FEBS Lett 586:4144–4147
30. Wormald MR, Petrescu AJ, Pao YL, Glithero A, Elliott T, Dwek RA (2002) Conformational studies of oligosaccharides and glycopeptides: complementarity of NMR, X-ray crystallography, and molecular modelling. Chem Rev 102:371–386
31. Gabius HJ, Andre S, Jimenez-Barbero J, Romero A, Solis D (2011) From lectin structure to functional glycomics: principles of the sugar code. Trends Biochem Sci 36:298–313
32. Kamiya Y, Yagi-Utsumi M, Yagi H, Kato K (2011) Structural and molecular basis of carbohydrate-protein interaction systems as potential therapeutic targets. Curr Pharm Des 17:1672–1684
33. Aebi M, Bernasconi R, Clerc S, Molinari M (2010) N-glycan structures: recognition and processing in the ER. Trends Biochem Sci 35:74–82
34. Kamiya Y, Satoh T, Kato K (2012) Molecular and structural basis for N-glycan-dependent determination of glycoprotein fates in cells. Biochim Biophys Acta 1820:1327–1337
35. Kato K, Kamiya Y (2007) Structural views of glycoprotein-fate determination in cells. Glycobiology 17:1031–1044
36. Regina Todeschini A, Hakomori SI (2008) Functional role of glycosphingolipids and gangliosides in control of cell adhesion, motility, and growth, through glycosynaptic microdomains. Biochim Biophys Acta 1780:421–433
37. Lopez PH, Schnaar RL (2009) Gangliosides in cell recognition and membrane protein regulation. Curr Opin Struct Biol 19:549–557

38. Ariga T, McDonald MP, Yu RK (2008) Role of ganglioside metabolism in the pathogenesis of Alzheimer's disease – a review. J Lipid Res 49:1157–1175
39. Matsuzaki K, Kato K, Yanagisawa K (2010) Abeta polymerization through interaction with membrane gangliosides. Biochim Biophys Acta 1801:868–877
40. Fadda E, Woods RJ (2010) Molecular simulations of carbohydrates and protein-carbohydrate interactions: motivation, issues and prospects. Drug Discov Today 15:596–609
41. Re S, Nishima W, Miyashita N, Sugita Y (2012) Conformational flexibility of N-glycans in solution studied by REMD simulations. Biophys Rev 4:179–187
42. Zhang Y, Yamaguchi T, Kato K (2013) New NMR tools for characterizing the dynamic conformations and interactions of oligosaccharides. Chem Lett 42:1455–1462
43. Rodriguez-Castaneda F, Haberz P, Leonov A, Griesinger C (2006) Paramagnetic tagging of diamagnetic proteins for solution NMR. Magn Reson Chem 44 Spec No:S10–S6
44. Bertini I, Luchinat C, Parigi G, Pierattelli R (2008) Perspectives in paramagnetic NMR of metalloproteins. Dalton Trans 3782–3790
45. Otting G (2010) Protein NMR, using paramagnetic ions. Annu Rev Biophys 39:387–405
46. Yamamoto S, Zhang Y, Yamaguchi T, Kameda T, Kato K (2012) Lanthanide-assisted NMR evaluation of a dynamic ensemble of oligosaccharide conformations. Chem Commun (Camb) 48:4752–4754
47. Zhang Y, Yamamoto S, Yamaguchi T, Kato K (2012) Application of paramagnetic NMR-validated molecular dynamics simulation to the analysis of a conformational ensemble of a branched oligosaccharide. Molecules 17:6658–6671